Supplement of Solid Earth, 8, 361–378, 2017
http://www.solid-earth.net/8/361/2017/
doi:10.5194/se-8-361-2017-supplement

Solid Earth
Open Access

Supplement of

Precise age for the Permian–Triassic boundary in South China from high-precision U-Pb geochronology and Bayesian age–depth modeling

Björn Baresel et al.

Correspondence to: Björn Baresel (bjoern@heldenepos.de)

Supplement S1: Samples

The Dongpan section is situated at 22°16'11.80"N and 107°41'31.30"E, north-east of Liuqiao. The Penglaitan section is situated at 23°41'8.4"N and 109°18'21.0"E, east of Laibin.

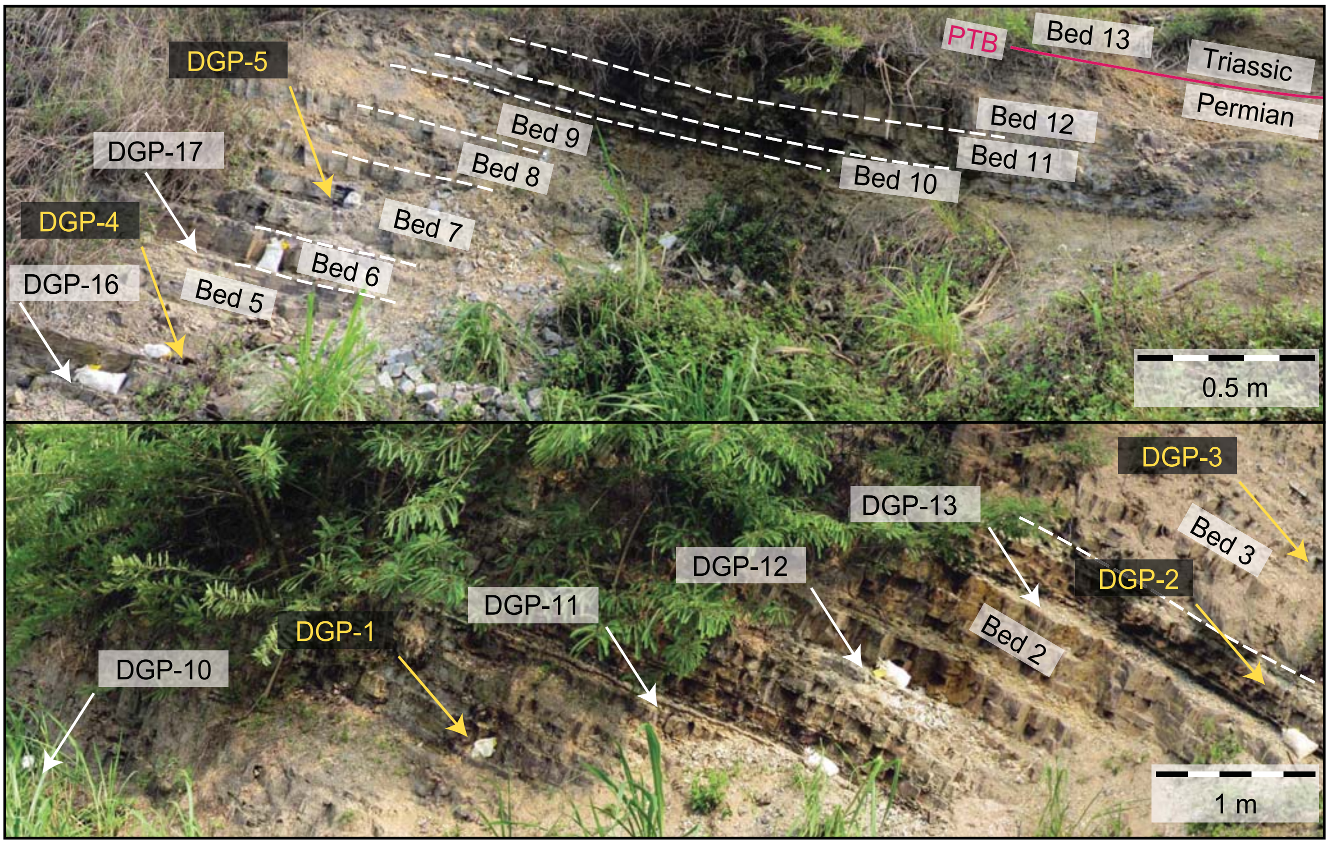

Figure S1. Studied volcanic ash beds (in black), radiolarian samples (in yellow), and their associated beds of the Changhsingian Dalong Formation at the Dongpan section. Both pictures present the continuous Dongpan section, where the upper picture is stratigraphically above the lower one. The Permian-Triassic boundary (PTB) in Dongpan is marked by the lithological boundary between the Permian Dalong Formation and the Triassic Ziyun Formation.

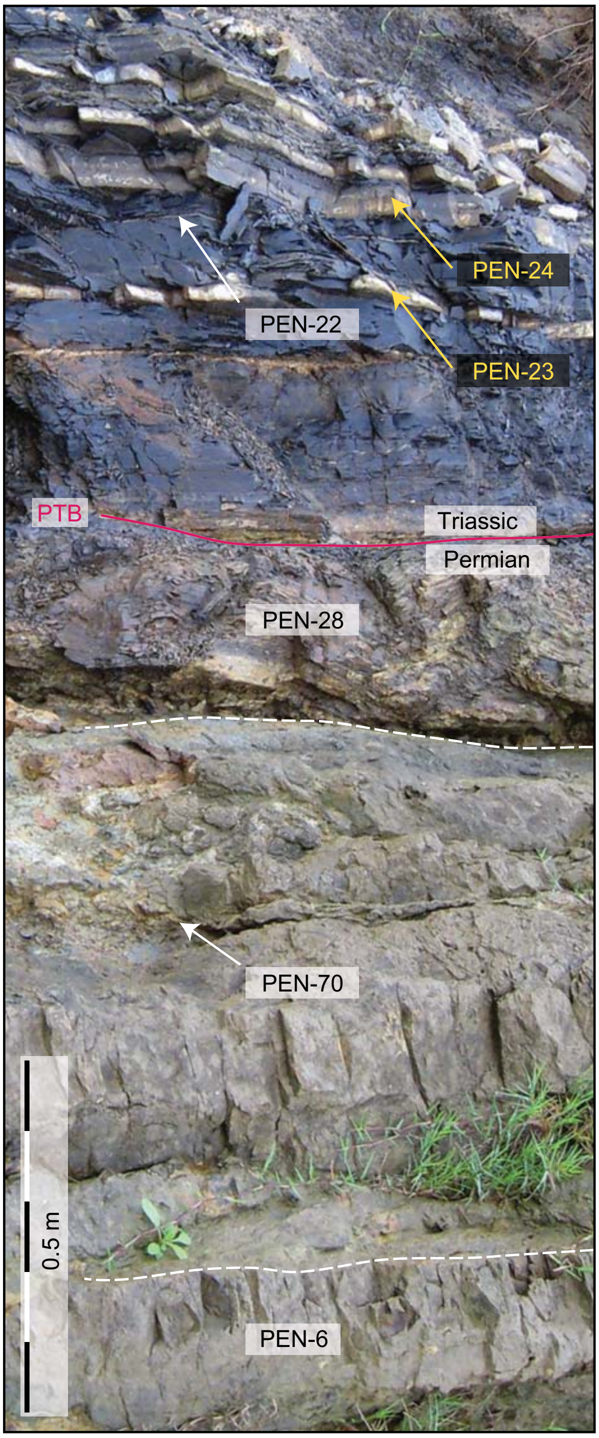

Figure S2. Studied volcanic ash beds and volcaniclastic sandstones (in black), and conodont samples (in yellow) of the Penglaitan section. The Permian-Triassic boundary (PTB) is marked by the lithological boundary between the Permian Dalong Formation and the Triassic Ziyun Formation.

Supplement S2: U-Pb zircon CA-ID-TIMS analysis

The samples were crushed and milled, and the powder was wet-sieved to remove the clay fraction. Heavy minerals were isolated using methylene iodide. Single zircons were microscopically inspected and euhedral crystals were picked for annealing at 900°C for ~48 h, followed by chemical abrasion with 40 % HF and trace HNO_3 in pressurized 200 µl Savillex mini-capsules at 180°C for 18 h to minimize Pb loss effects (Mattinson, 2005). Since Ovtcharova et al. (2015) still revealed apparent Pb loss in some zircon grains after 15 h of chemical abrasion, this study was optimized to the longer duration of 18 h to effectively overcome this obstacle.

After several washing steps with water, 6 N HCl, and 3 N HNO_3, single crystals were loaded in 200 µl Savillex capsules, spiked with ~4 mg of the EARTHTIME ^{202}Pb-^{205}Pb-^{233}U-^{235}U tracer solution (hereafter referred to as ET2535; Condon et al., 2015) and dissolved in ~70 µl 40 % HF and trace HNO_3 at 210°C for 48 h. After dissolution, samples were dried and re-dissolved in 6 N HCl at 180°C for 12 h, dried down again and re-dissolved in 3 N HCl. U and Pb were collected in 3 ml Savillex beakers after separation in a modified single 50 µl column anion exchange chemistry (Krogh, 1973) and dried down with a drop of 0.05 M H_3PO_4. They were loaded on a single outgassed Re filament with a Si-gel emitter modified from Gerstenberger and Haase (1997). Measurements of U and Pb isotopes were performed on a Thermo TRITON thermal ionization mass spectrometer utilizing the ET2535 tracer calibration version 3.0 defined by Condon et al. (2015). Pb isotopes were measured in dynamic mode on a MasCom secondary electron multiplier with a deadtime of 23 ns. Instrumental mass fractionation was corrected using the fractionation factor derived from the measured $^{202}Pb/^{205}Pb$ ratio relative to a true value of 0.99924. $BaPO_2$ interferences on mass 202 to 205 were corrected by determining $^{138}Ba^{31}P^{16}O^{16}O$ concentration on mass 201 assuming natural abundance of ^{138}Ba of 71.7 %. No correction was applied for isobaric interference of Tl on mass 205 (natural abundance of ^{205}Tl = 70.48 %, ^{203}Tl = 29.52 %) since routine check of the Re filaments yielded negligible concentrations on mass 203. U isotopes were measured in static mode on Faraday cups equipped with 10^{12} Ω resistors as UO_2^+ and measured ratios were corrected for isobaric interferences of $^{233}U^{18}O^{16}O$ on $^{235}U^{16}O^{16}O$ using $^{18}O/^{16}O$ of 0.0020, measured on large U500 loads, and for mass fractionation using the measured $^{233}U/^{235}U$ ratio relative to a value of 0.99506, assuming a sample $^{238}U/^{235}U$ ratio of 137.818 ± 0.045 (2σ; Hiess et al., 2012). Raw data were statistical filtered by using the Tripoli program, followed by data reduction including correct uncertainty propagation and online data visualization using U-Pb_Redux software (Bowring et al., 2011; McLean et al., 2011). U-Pb ratios and dates were calculated relative to a tracer $^{235}U/^{205}Pb$ ratio of 100.23 ± 0.046 % (2σ; Condon et al., 2015). All common Pb in the analyses was assumed to be procedural blank yielding a long-term average $^{206}Pb/^{204}Pb$ ratio of 18.469 ± 0.458, $^{207}Pb/^{204}Pb$ ratio of 15.471 ± 0.320, $^{208}Pb/^{204}Pb$ ratio of 38.011 ± 0.484 (uncertainties are given as 2σ) and an average of 0.52 pg during the course of this study.

Table S1. U-Pb single grain zircon dates and isotopic data.

Fraction and sample	Dates (Ma)				Disc. (%)	Composition			Isotopic Ratios						
	206Pb/238U *a °°	±2σ (absolute)	207Pb/235U *a	±2σ (absolute)	*b	Th/U *c	Pb (pg) *d	Pbc (pg) *e	206Pb/204Pb *f	206Pb/238U *g	±2σ (%)	207Pb/235U *g	±2σ (%)	207Pb/206Pb *g	±2σ (%)
Dongpan-18															
DGP 18.1	253.253	0.142	253.517	0.994	1.38	0.63	20.12	0.74	1618	0.0401	0.06	0.2836	0.44	0.0514	0.43
DGP 18.2	254.900	0.186	254.789	1.518	-0.10	0.59	11.39	0.66	1036	0.0403	0.07	0.2852	0.67	0.0513	0.66
DGP 18.3	257.274	0.689	257.017	2.366	-0.70	0.69	6.29	0.50	750	0.0407	0.27	0.2880	1.04	0.0513	0.99
DGP 18.4	255.159	0.364	254.345	2.676	-3.01	0.62	5.09	0.50	619	0.0404	0.15	0.2847	1.19	0.0512	1.16
DGP 18.5	254.752	0.568	253.430	1.742	-5.24	0.64	8.27	0.48	1025	0.0403	0.23	0.2835	0.78	0.0510	0.72
DGP 18.6	252.559	0.261	252.422	0.560	-0.22	0.64	35.48	0.51	4061	0.0399	0.11	0.2822	0.25	0.0513	0.21
DGP 18.7	256.837	0.275	256.141	2.378	-2.48	0.61	4.78	0.43	677	0.0406	0.11	0.2869	1.05	0.0512	1.03
DGP 18.8	253.456	0.184	253.776	1.592	1.61	0.58	13.80	0.86	973	0.0401	0.07	0.2839	0.71	0.0514	0.71
Dongpan-21															
DGP 21.2	252.677	0.241	252.499	0.494	-0.38	0.59	52.48	0.51	6089	0.0400	0.10	0.2823	0.22	0.0513	0.18
DGP 21.4	252.715	0.084	252.668	0.412	0.15	0.55	42.44	0.52	4883	0.0400	0.03	0.2825	0.18	0.0513	0.17
DGP 21.5	252.265	0.163	252.503	0.442	1.25	0.95	29.07	0.38	4114	0.0399	0.07	0.2823	0.20	0.0513	0.18
DGP 21.6	252.586	0.117	252.523	0.339	0.07	0.69	43.39	0.44	5721	0.0399	0.05	0.2824	0.15	0.0513	0.13
DGP 21.8	251.908	0.134	251.934	0.875	0.45	0.61	19.59	0.57	2053	0.0398	0.05	0.2816	0.39	0.0513	0.39
DGP 21.10	252.145	0.120	252.108	0.438	0.19	0.62	29.98	0.41	4356	0.0399	0.05	0.2818	0.20	0.0513	0.18
DGP 21.12	251.969	0.229	251.711	0.720	-0.73	0.67	26.37	0.46	3340	0.0398	0.09	0.2813	0.32	0.0512	0.25
DGP 21.13	251.975	0.077	252.032	0.715	0.58	0.52	17.62	0.49	2206	0.0398	0.03	0.2817	0.32	0.0513	0.33
DGP 21.14	252.240	0.157	252.369	0.850	0.84	0.77	13.19	0.40	1877	0.0399	0.06	0.2822	0.38	0.0513	0.37
DGP 21.15	251.929	0.080	251.955	0.694	0.46	0.53	19.68	0.54	2197	0.0398	0.03	0.2816	0.31	0.0513	0.31
DGP 21.17	251.945	0.113	251.963	0.480	0.42	0.56	39.56	0.63	3736	0.0398	0.05	0.2816	0.22	0.0513	0.20
DGP 21.18	251.896	0.230	251.998	1.429	0.75	0.61	11.49	0.61	1119	0.0398	0.09	0.2817	0.64	0.0513	0.60
DGP 21.20	251.976	0.074	252.081	0.523	0.77	0.57	29.35	0.59	2997	0.0398	0.03	0.2818	0.23	0.0513	0.23
DGP 21.21	251.940	0.172	252.109	1.486	1.02	0.62	10.01	0.58	1028	0.0398	0.07	0.2818	0.67	0.0513	0.65
Dongpan-17															
DGP 17.1	252.018	0.091	252.079	0.325	0.61	0.43	64.38	0.69	5792	0.0399	0.04	0.2818	0.15	0.0513	0.13
DGP 17.2	252.896	0.108	252.753	0.473	-0.23	0.50	36.24	0.51	4303	0.0400	0.04	0.2826	0.21	0.0513	0.19
DGP 17.3	251.899	0.096	252.006	0.514	0.80	0.44	31.56	0.60	3230	0.0398	0.04	0.2817	0.23	0.0513	0.22
DGP 17.4	251.871	0.120	252.189	0.623	1.64	0.44	25.52	0.56	2837	0.0398	0.05	0.2819	0.28	0.0514	0.26
DGP 17.5	251.990	0.131	251.620	0.505	-1.16	0.46	35.56	0.52	4195	0.0398	0.05	0.2812	0.23	0.0512	0.20
DGP 17.6	252.001	0.063	252.195	0.323	1.15	0.41	48.16	0.53	5661	0.0399	0.03	0.2819	0.14	0.0513	0.13
DGP 17.7	251.933	0.120	252.166	0.897	1.30	0.51	16.80	0.58	1773	0.0398	0.05	0.2819	0.40	0.0513	0.39
DGP 17.8	251.927	0.193	252.158	2.208	1.31	0.33	15.56	1.53	663	0.0398	0.08	0.2819	0.99	0.0513	0.99
DGP 17.9	251.929	0.101	252.328	0.493	1.96	0.41	30.66	0.54	3543	0.0398	0.04	0.2821	0.22	0.0514	0.21
DGP 17.10	252.003	0.210	252.585	0.637	2.67	0.41	20.82	0.51	2568	0.0399	0.08	0.2824	0.28	0.0514	0.27
DGP 17.11	251.938	0.118	252.124	0.330	1.13	0.36	42.18	0.49	5401	0.0398	0.05	0.2819	0.15	0.0513	0.13
DGP 17.12	251.866	0.158	251.890	0.478	0.46	0.45	29.58	0.52	3536	0.0398	0.06	0.2816	0.21	0.0513	0.20
Dongpan-16															
DGP 16.1	252.074	0.177	250.746	0.953	-5.34	0.37	20.74	0.73	1809	0.0399	0.07	0.2801	0.43	0.0510	0.41
DGP 16.3	252.008	0.113	251.757	1.091	-0.67	0.49	17.10	0.76	1388	0.0399	0.05	0.2814	0.49	0.0512	0.48
DGP 16.4	251.959	0.074	252.180	0.469	1.28	0.22	27.97	0.53	3469	0.0398	0.03	0.2819	0.21	0.0513	0.20

Table S1. continued.

Fraction and sample	Dates (Ma) 206Pb/238U *a°°	±2σ (absolute)	207Pb/235U *a	±2σ (absolute)	Disc. (%) *b	Composition Th/U *c	Pb (pg) *d	Pbc (pg) *e	Isotopic Ratios 206Pb/204Pb *f	206Pb/238U *g	±2σ (%)	207Pb/235U *g	±2σ (%)	207Pb/206Pb *g	±2σ (%)
DGP 16.5	252.018	0.149	251.175	1.164	-3.19	0.45	16.74	0.71	1456	0.0399	0.06	0.2807	0.52	0.0511	0.50
DGP 16.7	251.959	0.134	252.150	0.937	1.17	0.19	14.52	0.58	1673	0.0398	0.05	0.2819	0.42	0.0513	0.41
DGP 16.8	251.926	0.102	252.727	0.668	3.54	0.24	20.15	0.51	2607	0.0398	0.04	0.2826	0.30	0.0515	0.29
DGP 16.9	251.471	0.160	251.540	0.778	0.67	0.27	21.37	0.66	2095	0.0398	0.06	0.2811	0.35	0.0513	0.33
DGP 16.10	252.030	0.168	252.627	1.555	2.73	0.39	12.30	0.75	1041	0.0399	0.07	0.2825	0.70	0.0514	0.68
DGP 16.12	252.023	0.107	251.841	0.508	-0.35	0.26	24.27	0.49	3228	0.0399	0.04	0.2815	0.23	0.0512	0.21
DGP 16.13	251.897	0.158	252.166	0.703	1.47	0.27	18.84	0.51	2396	0.0398	0.06	0.2819	0.31	0.0514	0.30
Dongpan-13															
DGP 13.1	252.103	0.104	252.698	0.859	2.73	0.36	22.62	0.83	1727	0.0399	0.04	0.2826	0.38	0.0514	0.38
DGP 13.2	252.079	0.069	252.151	0.246	0.66	0.41	60.43	0.41	9091	0.0399	0.03	0.2819	0.11	0.0513	0.09
DGP 13.3	252.174	0.104	252.415	0.877	1.33	0.43	14.18	0.51	1738	0.0399	0.04	0.2822	0.39	0.0513	0.38
DGP 13.4	252.118	0.153	252.094	0.691	0.27	0.42	20.60	0.55	2331	0.0399	0.06	0.2818	0.31	0.0513	0.29
DGP 13.5	252.086	0.115	252.042	0.369	0.21	0.29	31.43	0.37	5516	0.0399	0.05	0.2817	0.17	0.0513	0.12
DGP 13.7	252.067	0.081	252.029	0.518	0.21	0.46	23.69	0.47	3095	0.0399	0.03	0.2817	0.23	0.0513	0.22
DGP 13.8	252.155	0.123	251.914	0.779	-0.63	0.45	18.88	0.57	2056	0.0399	0.05	0.2816	0.35	0.0512	0.34
Dongpan-12															
DGP 12.1	252.146	0.107	252.081	0.699	0.10	0.45	16.28	0.43	2346	0.0399	0.04	0.2818	0.31	0.0513	0.30
DGP 12.4	252.131	0.112	252.317	0.855	1.10	0.55	13.00	0.42	1864	0.0399	0.05	0.2821	0.38	0.0513	0.37
DGP 12.5	252.065	0.093	251.950	0.506	-0.09	0.35	25.11	0.44	3646	0.0399	0.04	0.2816	0.23	0.0513	0.21
DGP 12.6	252.032	0.112	252.101	0.777	0.63	0.54	13.84	0.41	2033	0.0399	0.05	0.2818	0.35	0.0513	0.33
DGP 12.7	252.159	0.090	252.536	0.804	1.86	0.50	12.34	0.39	1925	0.0399	0.04	0.2824	0.36	0.0514	0.35
DGP 12.8	252.102	0.094	252.185	0.586	0.66	0.69	19.34	0.40	2786	0.0399	0.04	0.2819	0.26	0.0513	0.25
DGP 12.9	252.224	0.148	251.873	0.892	-1.11	0.63	9.37	0.25	2253	0.0399	0.06	0.2815	0.40	0.0512	0.37
DGP 12.10	252.142	0.075	252.212	0.485	0.66	0.33	17.96	0.34	3371	0.0399	0.03	0.2820	0.22	0.0513	0.21
Dongpan-11															
DGP 11.1	252.458	0.208	252.299	1.063	-0.26	0.31	10.86	0.43	1626	0.0399	0.08	0.2821	0.48	0.0513	0.45
DGP 11.3	251.912	0.224	251.970	0.943	0.62	0.30	11.81	0.40	1889	0.0398	0.09	0.2817	0.42	0.0513	0.40
DGP 11.4	251.661	0.263	251.688	0.952	0.47	0.48	12.56	0.39	1957	0.0398	0.11	0.2813	0.43	0.0513	0.39
DGP 11.5	252.924	0.352	251.794	3.262	-4.43	0.43	2.37	0.31	498	0.0400	0.14	0.2814	1.46	0.0511	1.44
DGP 11.6	251.861	0.202	251.725	1.029	-0.17	0.29	11.14	0.43	1692	0.0398	0.08	0.2813	0.46	0.0513	0.45
DGP 11.7	252.881	0.571	252.626	6.500	-0.68	0.48	1.78	0.46	253	0.0400	0.23	0.2825	2.91	0.0513	2.88
DGP 11.8	252.039	0.210	251.722	1.798	-0.91	0.27	5.43	0.36	982	0.0399	0.09	0.2813	0.81	0.0512	0.78
DGP 11.10	251.884	0.274	252.117	2.953	1.32	0.31	5.30	0.66	528	0.0398	0.11	0.2818	1.32	0.0513	1.31
DGP 11.11	252.635	0.218	252.640	2.345	0.39	0.44	5.50	0.54	644	0.0400	0.09	0.2825	1.05	0.0513	1.04
DGP 11.12	252.155	0.257	252.014	2.254	-0.21	0.41	6.27	0.55	723	0.0399	0.10	0.2817	1.01	0.0513	0.99
DGP 11.14	252.580	0.316	252.776	3.295	1.16	0.35	4.95	0.59	545	0.0399	0.13	0.2827	1.47	0.0513	1.44
Dongpan-10															
DGP 10.1	252.088	0.150	251.900	0.762	-0.40	0.40	19.51	0.51	2402	0.0399	0.06	0.2816	0.34	0.0512	0.32
DGP 10.4	252.126	0.317	252.075	2.243	0.16	0.44	6.97	0.62	708	0.0399	0.13	0.2818	1.00	0.0513	0.99
DGP 10.5	252.142	0.121	252.084	0.815	0.14	0.38	11.87	0.38	1965	0.0399	0.05	0.2818	0.37	0.0513	0.35
DGP 10.6	252.770	0.183	252.896	1.847	0.87	0.45	4.97	0.39	807	0.0400	0.07	0.2828	0.82	0.0513	0.82

Table S1. continued.

Fraction and sample	Dates (Ma) 206Pb/238U *a°°	±2σ (absolute)	207Pb/235U *a	±2σ (absolute)	Disc. (%) *b	Composition Th/U *c	Pb (pg) *d	Pbc (pg) *e	Isotopic Ratios 206Pb/204Pb *f	206Pb/238U *g	±2σ (%)	207Pb/235U *g	±2σ (%)	207Pb/206Pb *g	±2σ (%)
DGP 10.7	252.147	0.091	252.590	0.708	2.13	0.40	14.72	0.42	2199	0.0399	0.04	0.2824	0.32	0.0514	0.31
DGP 10.8	252.769	0.204	252.740	1.368	0.25	0.42	8.93	0.48	1180	0.0400	0.08	0.2826	0.61	0.0513	0.59
DGP 10.9	252.254	0.242	252.244	1.725	0.33	0.39	6.12	0.43	904	0.0399	0.10	0.2820	0.77	0.0513	0.76
DGP 10.11	252.366	0.181	252.211	1.025	-0.26	0.43	10.91	0.41	1669	0.0399	0.07	0.2820	0.46	0.0513	0.44
DGP 10.12	252.201	0.159	252.379	0.861	1.06	0.55	12.49	0.42	1802	0.0399	0.06	0.2822	0.39	0.0513	0.37
DGP 10.13	252.826	0.424	252.481	2.031	-1.06	0.47	5.98	0.40	933	0.0400	0.17	0.2823	0.91	0.0512	0.86
Penglaitan-22															
PEN 22.2	251.909	0.073	251.819	0.444	0.00	0.44	36.92	0.50	4573	0.0398	0.03	0.2815	0.20	0.0513	0.20
PEN 22.3	251.405	0.174	251.671	0.358	1.44	0.43	46.73	0.53	5494	0.0398	0.07	0.2813	0.16	0.0513	0.13
PEN 22.4	251.895	0.080	252.071	0.360	1.09	0.35	38.18	0.46	5207	0.0398	0.03	0.2818	0.16	0.0513	0.14
PEN 22.6	251.910	0.055	252.004	0.366	0.77	0.28	29.59	0.46	4155	0.0398	0.02	0.2817	0.16	0.0513	0.16
PEN 22.7	251.964	0.237	251.667	1.108	-0.86	0.48	13.37	0.51	1614	0.0398	0.10	0.2813	0.50	0.0512	0.46
PEN 22.8	252.166	0.123	252.092	1.220	0.10	0.17	8.09	0.44	1248	0.0399	0.05	0.2818	0.55	0.0513	0.54
PEN 22.9	252.166	0.123	252.210	1.229	0.53	0.55	13.03	0.63	1252	0.0399	0.05	0.2820	0.55	0.0513	0.54
PEN 22.10	251.939	0.156	252.332	1.313	1.93	0.51	14.37	0.72	1229	0.0398	0.06	0.2821	0.59	0.0514	0.57
PEN 22.11	251.891	0.082	251.861	0.715	0.25	0.40	20.94	0.62	2139	0.0398	0.03	0.2815	0.32	0.0513	0.31
PEN 22.12	251.913	0.157	251.527	0.818	-1.19	0.18	6.21	0.14	2866	0.0398	0.06	0.2811	0.37	0.0512	0.33
PEN 22.13	251.923	0.205	251.163	1.490	-2.82	0.35	4.24	0.14	1895	0.0398	0.08	0.2806	0.67	0.0511	0.63
Penglaitan-28															
PEN 28.1	252.511	0.198	251.772	1.001	-2.75	0.60	18.86	0.67	1668	0.0399	0.08	0.2814	0.45	0.0511	0.43
PEN 28.2	252.078	0.083	252.151	0.760	0.64	0.59	22.29	0.64	2081	0.0399	0.03	0.2819	0.34	0.0513	0.34
PEN 28.3	252.057	0.106	252.080	0.597	0.43	0.65	25.69	0.52	2916	0.0399	0.04	0.2818	0.27	0.0513	0.25
PEN 28.4	252.096	0.086	252.096	0.536	0.35	0.57	25.37	0.52	2913	0.0399	0.03	0.2818	0.24	0.0513	0.23
PEN 28.5	252.364	0.156	252.603	1.227	1.25	0.96	10.94	0.47	1277	0.0399	0.06	0.2825	0.55	0.0513	0.54
PEN 28.6	252.045	0.119	251.936	1.366	-0.10	0.58	14.53	0.82	1074	0.0399	0.05	0.2816	0.61	0.0513	0.62
PEN 28.7	251.989	0.144	252.023	0.676	0.49	0.56	28.93	0.62	2784	0.0399	0.06	0.2817	0.30	0.0513	0.28
PEN 28.8	252.174	0.367	251.129	2.321	-4.10	0.59	4.11	0.37	680	0.0399	0.15	0.2806	1.04	0.0511	1.02
PEN 28.9	252.430	0.286	252.213	1.763	-0.56	0.69	6.03	0.40	898	0.0399	0.12	0.2820	0.79	0.0512	0.77
PEN 28.10	252.413	0.245	252.919	2.130	2.32	0.80	6.63	0.53	724	0.0399	0.10	0.2829	0.95	0.0514	0.94
PEN 28.11	251.994	0.167	252.168	0.996	1.04	0.63	10.75	0.39	1621	0.0399	0.07	0.2819	0.45	0.0513	0.43
PEN 28.12	252.403	0.284	252.540	1.982	0.89	0.61	6.77	0.52	789	0.0399	0.11	0.2824	0.89	0.0513	0.87
PEN 28.13	253.090	0.375	252.838	2.764	-0.69	0.64	3.87	0.42	559	0.0400	0.15	0.2828	1.24	0.0513	1.22
Penglaitan-70															
PEN 70.1	253.371	0.165	253.002	1.461	-1.21	0.87	16.24	0.87	1054	0.0401	0.07	0.2830	0.65	0.0512	0.64
PEN 70.2	252.917	0.220	252.968	0.711	0.54	0.61	36.74	0.98	2233	0.0400	0.09	0.2829	0.32	0.0513	0.30
PEN 70.3	252.778	0.270	252.955	1.111	1.04	0.64	17.72	0.65	1618	0.0400	0.11	0.2829	0.50	0.0513	0.47
PEN 70.4	252.137	0.200	252.078	0.967	0.10	0.62	16.95	0.57	1769	0.0399	0.08	0.2818	0.43	0.0513	0.41
PEN 70.6	252.519	0.125	252.436	0.510	0.01	0.57	34.71	0.65	3223	0.0399	0.05	0.2822	0.23	0.0513	0.22
PEN 70.7	253.079	0.283	253.701	1.493	2.70	1.22	20.94	1.04	1039	0.0400	0.11	0.2838	0.67	0.0515	0.64
PEN 70.8	253.309	0.231	253.620	1.294	1.55	0.81	13.88	0.67	1180	0.0401	0.09	0.2837	0.58	0.0514	0.57
PEN 70.9	252.156	0.147	252.327	0.404	1.03	0.64	52.32	0.56	5516	0.0399	0.06	0.2821	0.18	0.0513	0.16

Table S1. continued.

Fraction and	Dates (Ma)					Composition			Isotopic Ratios						
	206Pb/238U	±2σ	207Pb/235U	±2σ	Disc. (%)	Th/U	Pb (pg)	Pbc (pg)	206Pb/204Pb	206Pb/238U	±2σ	207Pb/235U	±2σ	207Pb/206Pb	±2σ
sample	*a °°	(absolute)	*a	(absolute)	*b	*c	*d	*e	*f	*g	(%)	*g	(%)	*g	(%)
PEN 70.10	253.036	0.339	253.063	0.777	0.45	0.59	19.61	0.52	2261	0.0400	0.14	0.2830	0.35	0.0513	0.31
PEN 70.11	251.994	0.169	252.052	0.446	0.56	0.69	51.50	0.66	4508	0.0399	0.07	0.2818	0.20	0.0513	0.17
PEN 70.12	252.153	0.230	252.159	1.201	0.37	0.60	13.80	0.51	1616	0.0399	0.09	0.2819	0.54	0.0513	0.51
PEN 70.13	253.341	0.128	253.340	1.121	0.31	0.77	11.91	0.51	1345	0.0401	0.05	0.2834	0.50	0.0513	0.49
PEN 70.14	253.136	0.228	253.163	1.951	0.43	0.70	13.35	0.93	846	0.0400	0.09	0.2832	0.87	0.0513	0.86
PEN 70.16	252.515	0.105	252.243	0.348	-0.72	0.27	16.42	0.16	6680	0.0399	0.04	0.2820	0.16	0.0512	0.13
PEN 70.17	252.215	0.350	251.974	0.528	-0.65	0.61	15.81	0.17	5572	0.0399	0.14	0.2817	0.24	0.0512	0.17
PEN 70.19	252.166	0.127	252.256	0.253	0.67	0.86	43.54	0.28	8650	0.0399	0.05	0.2820	0.11	0.0513	0.09
PEN 70.20	252.676	0.258	252.493	0.385	-0.39	0.50	20.85	0.16	7842	0.0400	0.10	0.2823	0.17	0.0513	0.12
PEN 70.22	252.062	0.274	251.239	0.831	-3.11	0.55	19.83	0.32	3682	0.0399	0.11	0.2807	0.37	0.0511	0.27
Penglaitan-6															
PEN 6.1	252.889	0.295	254.066	3.159	4.87	0.59	9.05	1.14	486	0.0400	0.12	0.2843	1.41	0.0516	1.39
PEN 6.2	253.231	0.184	253.518	1.674	1.48	0.58	6.96	0.45	926	0.0401	0.07	0.2836	0.75	0.0514	0.73
PEN 6.3	253.745	0.241	253.643	2.159	-0.09	0.67	6.16	0.49	740	0.0401	0.10	0.2838	0.96	0.0513	0.94
PEN 6.4	252.679	0.102	253.035	0.688	1.76	0.59	19.60	0.48	2435	0.0400	0.04	0.2830	0.31	0.0514	0.30
PEN 6.5	252.123	0.099	252.325	0.612	1.16	0.56	26.32	0.52	3029	0.0399	0.04	0.2821	0.27	0.0513	0.25
PEN 6.7	252.754	0.240	254.068	2.670	5.35	0.70	7.16	0.74	575	0.0400	0.10	0.2843	1.19	0.0516	1.18
PEN 6.10	253.199	0.319	254.546	2.200	5.41	1.00	5.97	0.45	722	0.0400	0.13	0.2849	0.98	0.0516	0.96
PEN 6.12	252.793	0.229	252.635	1.453	-0.30	0.59	8.32	0.46	1080	0.0400	0.09	0.2825	0.65	0.0513	0.63
PEN 6.13	252.728	0.187	253.169	1.293	2.09	0.62	9.76	0.49	1193	0.0400	0.08	0.2832	0.58	0.0514	0.57
PEN 6.14	252.550	0.205	252.547	1.986	0.33	0.57	6.68	0.51	791	0.0399	0.08	0.2824	0.89	0.0513	0.87
PEN 6.15	252.161	0.237	251.253	1.230	-3.51	0.68	6.78	0.19	2134	0.0399	0.10	0.2808	0.55	0.0511	0.52
PEN 6.16	252.567	0.183	252.405	1.351	-0.36	0.93	5.33	0.22	1358	0.0399	0.07	0.2822	0.60	0.0513	0.57
PEN 6.17	252.862	0.144	252.540	1.143	-0.97	0.51	6.78	0.28	1464	0.0400	0.06	0.2824	0.51	0.0512	0.49
PEN 6.18	252.172	0.191	249.752	0.886	-10.60	0.41	8.95	0.19	2959	0.0399	0.08	0.2789	0.40	0.0507	0.31
PEN 6.19	252.581	0.145	252.136	0.535	-1.50	0.63	12.68	0.20	3724	0.0399	0.06	0.2819	0.24	0.0512	0.23

a Isotopic dates calculated using the decay constants λ238 = 1.55125E-10 and λ235 = 9.8485E-10 (Jaffey et al., 1971).
b % discordance = 100 - (100 * (206Pb/238U date) / (207Pb/206Pb date)).
c Th contents calculated from radiogenic 208Pb and the 207Pb/206Pb date of the sample, assuming concordance between U-Th and Pb systems.
d Total mass of radiogenic Pb.
e Total mass of common Pb.
f Measured ratio corrected for fractionation and spike contribution only.
g Measured ratio corrected for fractionation, tracer and blank.
°° Corrected for initial Th/U disequilibrium using radiogenic 208Pb and Th/U_{magma} = 3.00.
* Samples marked in red are from a previous study (Baresel et al., 2016).

Baresel, B., D'Abzac, F.X., Bucher, H., and Schaltegger, U.: High-precision time-space correlation through coupled apatite and zircon tephrochronology: an example from the Permian-Triassic boundary in South China. Geology, 45, 83–86, doi:10.1130/g38181.1, 2016.

Bowring, J.F., McLean, N.M., and Bowring, S.A.: Engineering cyber infrastructure for U-Pb geochronology: tripoli and U-Pb_Redux. Geochem. Geophy. Geosy., 12, Q0AA19, doi:10.1029/2010GC003479, 2011.

Condon, D.J., Schoene, B., McLean, N.M., Bowring, S.A., and Parrish, R.R.: Metrology and traceability of U-Pb isotope dilution geochronology (EARTHTIME Tracer Calibration Part I). Geochim. Cosmochim. Ac., 164, 464–480, doi:10.1016/j.gca.2015.05.026, 2015.

Gerstenberger, H., and Haase, G.: A highly effective emitter substance for mass spectrometric Pb isotope ratio determination. Chem. Geol., 136, 309–312, doi:10.1016/S0009-2541(96)00033-2, 1997.

Hiess, J., Condon, D.J., McLean, N.M., and Noble, S.R.: $^{238}U/^{235}U$ Systematics in terrestrial uranium-bearing minerals. Science, 335, 1610–1614, doi:10.1126/science.1215507, 2012.

Jaffey, A.H., Flynn, K.F., Glendenin, L.E., Bentley, W.C., and Essling, A.M.: Precision measurements of half-lives and specific activities of ^{235}U and ^{238}U. Phys. Rev. C, 4, 1889–1906, doi:10.1103/physrevc.4.1889, 1971.

Krogh, T.E.: A low contamination method for hydrothermal decomposition of zircon and extraction of U and Pb for isotopic age determination. Geochim. Cosmochim. Ac., 37, 485–494, doi:10.1016/0016-7037(73)90213-5, 1973.

Mattinson, J.M.: Zircon U-Pb chemical abrasion ("CA-TIMS") method: combined annealing and multi-step partial dissolution analysis for improved precision and accuracy of zircon ages. Chem. Geol., 220, 47–66, doi:10.1016/j.chemgeo.2005.03.011, 2005.

McLean, N.M., Bowring, J.F., and Bowring, S.A.: An algorithm for U-Pb isotope dilution data reduction and uncertainty propagation. Geochem. Geophy. Geosy., 12, Q0AA18, doi:10.1029/2010GC003478, 2011.

Ovtcharova, M., Goudemand, N., Hammer, O., Guodun, K., Cordey, F., Galfetti, T., Schaltegger, U., and Bucher, H.: Developing a strategy for accurate definition of a geological boundary through radio-isotopic and biochronological dating: The Early–Middle Triassic boundary (South China). Earth-Sci. Rev., 146, 65–76, doi:10.1016/j.earscirev.2015.03.006, 2015.

Supplement S3: Bayesian method Bchron modeling

The age-depth models of Dongpan, Penglaitan and Meishan have been run under the free and open-source software RStudio Desktop version 1.0.44 using the free Bchron R package version 4.1.1 (Haslett and Parnell, 2008; Parnell et al., 2008). Detailed documentation of available program commands is provided in the embedded description file of the Bchron package.

Bchron R scripts

Dongpan model

Input parameter:	"id"	age [ka]	1s [ka]	position [cm]	thickness [cm]	"calCurves"
	"DGP-18"	252560	260	52	2	"normal"
	"DGP-21"	251953	19	93	2	"normal"
	"DGP-17"	251956	17	368	8	"normal"
	"DGP-16"	251978	20	426	4	"normal"
	"DGP-13"	252101	19	743	6	"normal"
	"DGP-12"	252121	18	833	5	"normal"
	"DGP-11"	251924	48	894	5	"normal"
	"DGP-10"	252170	28	1075	2	"normal"

Script:

```
data (Dongpan)
DGPOut=Bchronology(ages=Dongpan$ages,ageSds=Dongpan$ageSds,
calCurves=Dongpan$calCurves,positions=Dongpan$position,positionThicknesses=Dongpan$thickness,
ids=Dongpan$id,predictPositions=seq(0,1075,by=1),iterations=10000,extractDate=251700)
plot(DGPOut,main="Dongpan",xlab='Age (Ma)',ylab='Depth (cm)',las=1)
predictAges=predict(DGPOut, newPositions=c(100,415),newPositionThicknesses=c(0,0))
summary(DGPOut)
summary(DGPOut, type='convergence')
summary(DGPOut, type='outliers')
```

Dongpan model (rescaled)

Input parameter:	"id"	age [ka]	1s [ka]	position [cm]	thickness [cm]	"calCurves"
	"DGP-18"	252560	260	50	0	"normal"
	"DGP-21"	251953	19	89	0	"normal"
	"DGP-17"	251956	17	356	0	"normal"
	"DGP-16"	251978	20	410	0	"normal"
	"DGP-13"	252101	19	682	0	"normal"

"DGP-12"	252121	18	767	0	"normal"
"DGP-11"	251924	48	819	0	"normal"
"DGP-10"	252170	28	988	0	"normal"

Script:

```
data (Dongpan)
DGPOut=Bchronology(ages=Dongpan$ages,ageSds=Dongpan$ageSds,
calCurves=Dongpan$calCurves,positions=Dongpan$position,positionThicknesses=Dongpan$thickness,
ids=Dongpan$id,predictPositions=seq(0,988,by=1),iterations=10000,extractDate=251700)
plot(DGPOut,main="Dongpan",xlab='Age (Ma)',ylab='Depth (cm)',las=1)
predictAges=predict(DGPOut, newPositions=c(96,399),newPositionThicknesses=c(0,0))
summary(DGPOut)
summary(DGPOut, type='convergence')
summary(DGPOut, type='outliers')
```

Penglaitan model

Input parameter:

"id"	age [ka]	1s [ka]	position [cm]	thickness [cm]	"calCurves"
"PEN-22"	251907	17	53	1	"normal"
"PEN-28"	252062	22	131	1	"normal"
"PEN-70"	252125	35	161	1	"normal"
"PEN-6"	252137	41	209	1	"normal"

Script:

```
data (Penglaitan)
PENOut=Bchronology(ages=Penglaitan$ages,ageSds=Penglaitan$ageSds,
calCurves=Penglaitan$calCurves,positions=Penglaitan$position,
positionThicknesses=Penglaitan$thickness,ids=Penglaitan$id,
predictPositions=seq(0,212,by=1),iterations=10000,extractDate=251700)
plot(PENOut,main="Penglaitan",xlab='Age (Ma)',ylab='Depth (cm)',las=1)
predictAges=predict(PENOut, newPositions=c(100),newPositionThicknesses=c(0))
summary(PENOut)
summary(PENOut, type='convergence')
summary(PENOut, type='outliers')
```

Penglaitan model (rescaled)

Input parameter:

"id"	age [ka]	1s [ka]	position [cm]	thickness [cm]	"calCurves"
"PEN-22"	251907	17	53	0	"normal"
"PEN-28"	252062	22	131	0	"normal"

"PEN-70"	252125	35	157	0	"normal"
"PEN-6"	252137	41	205	0	"normal"

Script:

```
data (Penglaitan)
PENOut=Bchronology(ages=Penglaitan$ages,ageSds=Penglaitan$ageSds,
calCurves=Penglaitan$calCurves,positions=Penglaitan$position,
positionThicknesses=Penglaitan$thickness,ids=Penglaitan$id,
predictPositions=seq(0,131,by=1),iterations=10000,extractDate=251700)
plot(PENOut,main="Penglaitan",xlab='Age (Ma)',ylab='Depth (cm)',las=1)
predictAges=predict(PENOut, newPositions=c(99),newPositionThicknesses=c(0))
summary(PENOut)
summary(PENOut, type='convergence')
summary(PENOut, type='outliers')
```

Meishan model (rescaled)

Input parameter:

"id"	age [ka]	1s [ka]	position [cm]	thickness [cm]	"calCurves"
"BED 34"	251495	32	1	0	"normal"
"BED 33"	251583	43	420	0	"normal"
"BED 28"	251880	16	580	0	"normal"
"BED 25"	251941	19	602	0	"normal"
"BED 22"	252104	45	1035	0	"normal"

Script:

```
data (Meishan)
MEIOut=Bchronology(ages=Meishan$ages,ageSds=Meishan$ageSds,
calCurves=Meishan$calCurves,positions=Meishan$position,
positionThicknesses=Meishan$thickness,ids=Meishan$id,
predictPositions=seq(0,1040,by=1),iterations=10000,extractDate=251200)
plot(MEIOut,main="Meishan",xlab='Age (Ma)',ylab='Depth (cm)',las=1)
predictAges=predict(MEIOut, newPositions=c(602),newPositionThicknesses=c(0))
summary(MEIOut)
summary(MEIOut, type='convergence')
summary(MEIOut, type='outliers')
```

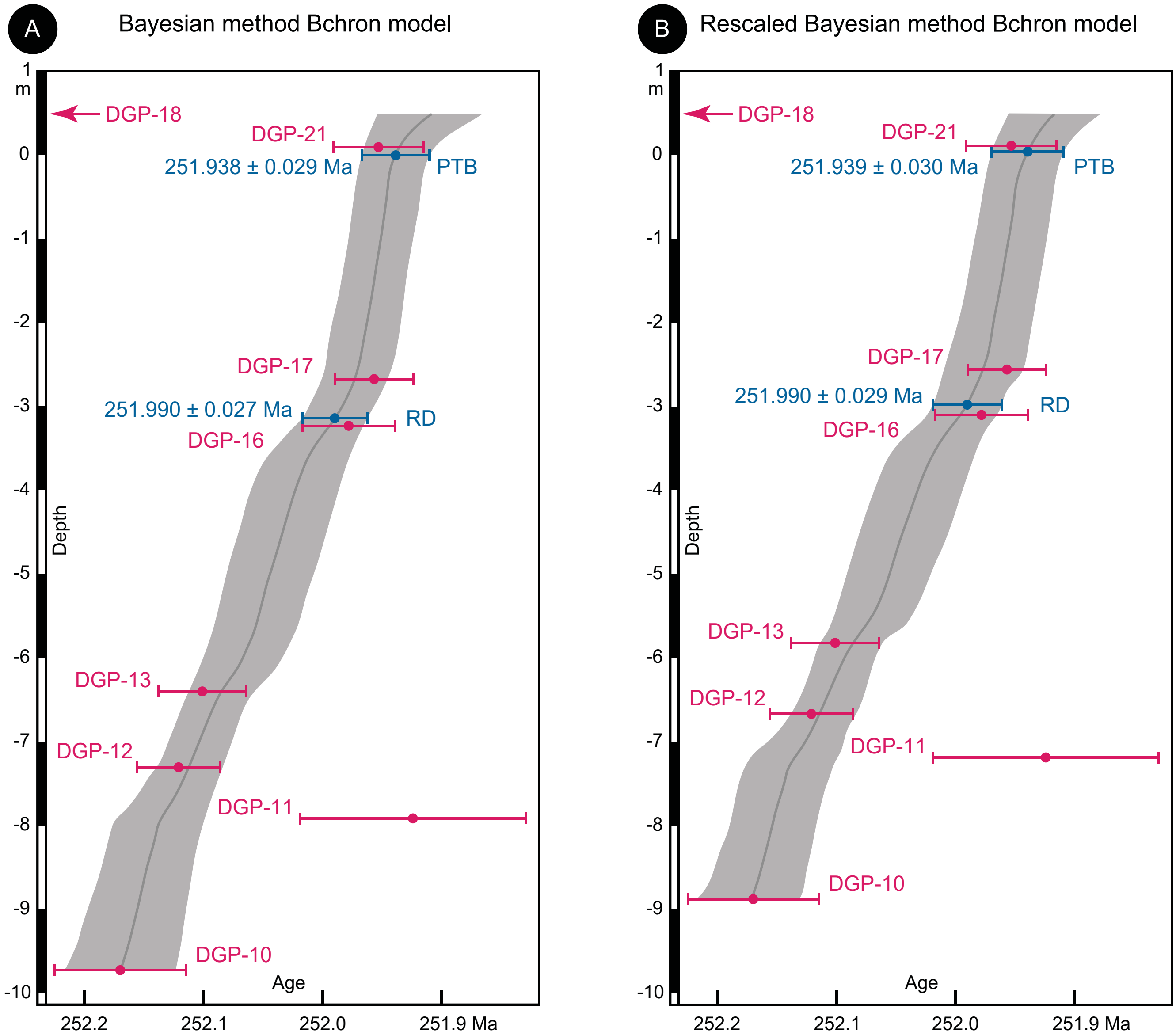

Figure S3. Comparison of the two different Bchron models for Dongpan using **(a)** the real stratigraphic thickness of each volcanic ash and **(b)** the rescaled lithostratigraphy to remove the thickness of the volcanic horizons. Each age-depth model is presented with its median (middle grey line) and its associated 95 % confidence interval (grey area). Radioisotopic dates, used in the age-depth models, together with their uncertainty (red horizontal bars) are presented as $^{206}Pb/^{238}U$ weighted mean dates of the volcanic ash beds. U-Pb data of DGP-21 is taken from Baresel et al. (2016). Predicted dates (blue horizontal bars) for the onset of the radiolarian decline (RD) and the Permian-Triassic Boundary (PTB) in Dongpan are calculated with their associated uncertainty using the different age-depth models.

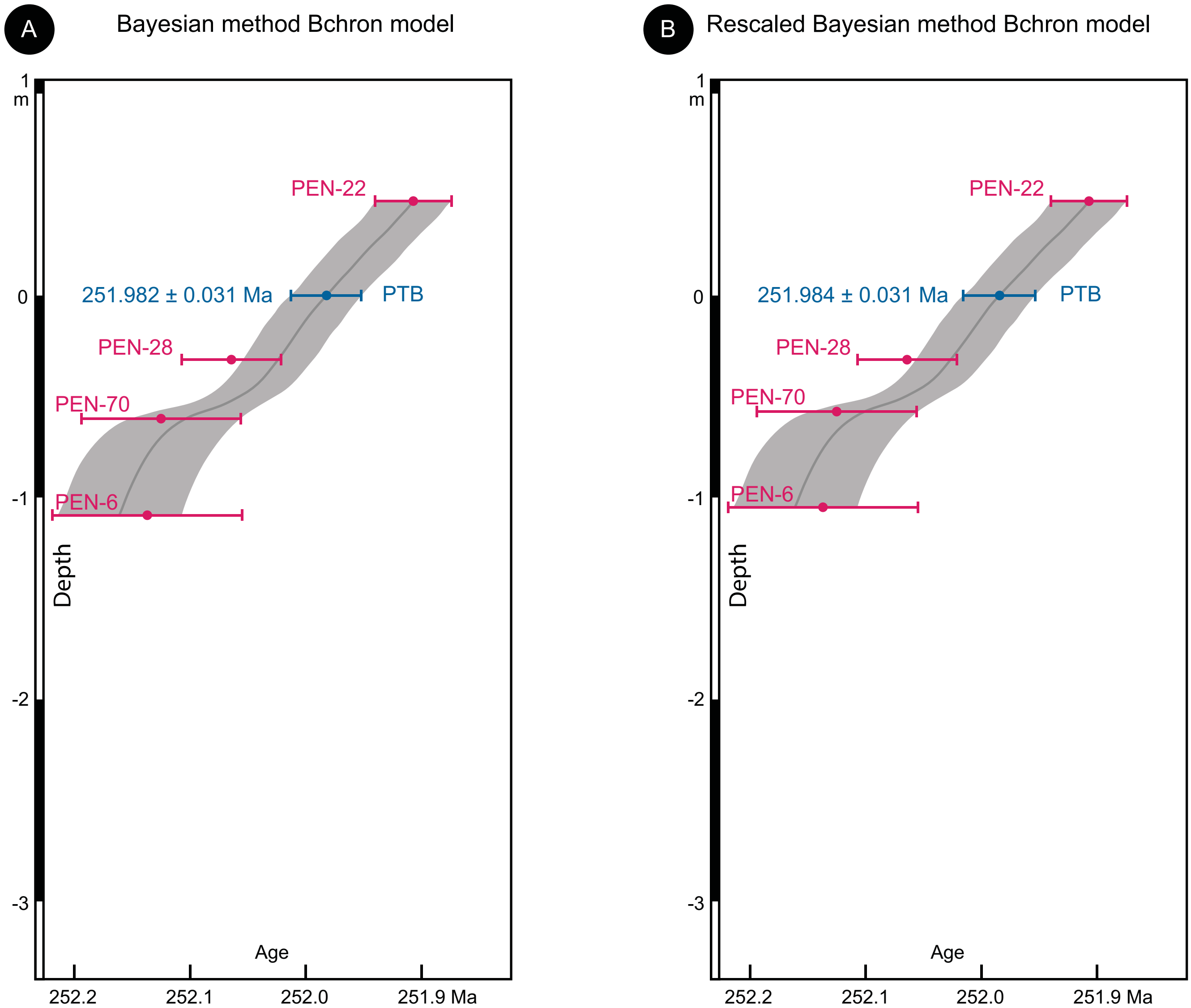

Figure S4. Comparison of the two different Bchron models for Penglaitan using **(a)** the real stratigraphic thickness of each volcanic ash and **(b)** the rescaled lithostratigraphy to remove the thickness of the volcanic horizons. Each age-depth model is presented with its median (middle grey line) and its associated 95 % confidence interval (grey area). Radioisotopic dates, used in the age-depth models, together with their uncertainty (red horizontal bars) are presented as $^{206}Pb/^{238}U$ weighted mean dates of the volcanic ash beds. U-Pb data of PEN-22 and PEN-28 are taken from Baresel et al. (2016). Predicted dates (blue horizontal bars) for the Permian-Triassic Boundary (PTB) in Penglaitan are calculated with their associated uncertainty using the different age-depth models.

Baresel, B., D'Abzac, F.X., Bucher, H., and Schaltegger, U.: High-precision time-space correlation through coupled apatite and zircon tephrochronology: an example from the Permian-Triassic boundary in South China. Geology, 45, 83–86, doi:10.1130/g38181.1, 2016.

Haslett, J., and Parnell, A.: A simple monotone process with application to radiocarbon-dated depth chronologies. J. Roy. Stat. Soc. C-App., 57, 399–418, doi:10.1111/j.1467-9876.2008.00623.x, 2008.

Parnell, A.C., Haslett, J., Allen, J.R.M., Buck, C.E., and Huntley, B.: A flexible approach to assessing synchroneity of past events using Bayesian reconstructions of sedimentation history. Quat. Sci. Rev., 27, 1872–1885, doi:10.1016/j.quascirev.2008.07.009, 2008.

Supplement S4: Dongpan radiolarians

Feng et al. (2007) suggested that radiolarian faunas underwent two successive extinction phases in Dongpan. Their first radiolarian crisis (FRC) occurs in bed 6 and their second radiolarian crisis (SRC) in bed 8 (Fig. 7). Hence, these authors proposed that the decline of radiolarians preceded a late Permian mass extinction (LPME; Fig. 7) placed in bed 9 on the basis of impoverished brachiopod, foraminifera and ostracod faunas (He et al., 2007; Yin et al., 2007) and of a negative excursion of the $\delta^{13}C_{org}$ record (Zhang et al., 2006). Subsequently, Feng and Algeo (2014) published a new radiolarian diversity curve showing the initiation of a protracted decline ("preliminary extinction": PE) starting in the middle part of bed 5. The second radiolarian crisis as initially recognized by Feng et al. (2007) is no longer visible in this progressive diversity reduction at the species level.

As radiolarians are well known to be highly sensitive to selective preservation bias, the comparison of this apparent diversity change with excess SiO_2 brings further insights. Shen et al. (2012) plotted excess SiO_2 along the Dongpan section but it is unclear how much biogenic or volcanogenic silica respectively contributed to these values. Above bed 9, Shen et al. (2012) also indicate absence of kaolinite in the clay fraction, suggesting that a lack of volcaniclastic input did contribute to the low levels of excess SiO_2. This drop of kaolinite and excess SiO_2 corresponds to the LPME of Feng et al. (2007) and to a lesser degree to the "main extinction" (ME) of Feng and Algeo (2014), which they placed in bed 8. The coincidence between the drop of excess SiO_2 and the LPME and/or the ME does not enable distinguishing a real extinction event of the radiolarians from a selective preservation bias.

Feng and Algeo (2014) interpreted the onset of the radiolarian decline in bed 5 as being morphologically selective, with long-spined species of the orders *Spumellaria* and *Entactinaria* preferentially going extinct relative to short-spined species. However, such a statement requires precise investigation of the effects of diagenesis on a bed by bed basis, as post-depositional dissolution can be extremely heterogeneous and guided by minor differences of available amount of SiO_2 in each bed. The model proposed by Feng and Algeo (2014) for the evolution of radiolarian-bearing rocks calls upon changes of oceanic redox conditions during the Permo-Triassic transition. This model is based on the assumption that Permian radiolarians can be divided into three paleoecological assemblages based on proportions between four orders (*Entactinaria*, *Spumellaria*, *Latentifistularia* and *Albaillellaria*), each restricted to shallow-, intermediate-, and deep-water environments. Dongpan was one of the main examples used to support the claim that radiolarians were differentially affected around the PTB events by an expansion of the oxygen minimum zone (OMZ). According to their scenario, deep-water taxa declined earlier than shallow-water taxa as a result of an expansion of the OMZ. This ecological model of radiolarian stratification with partial mutual taxonomic exclusion is only loosely supported by well-constrained Late Permian data worldwide and is not supported when compared to the present-day planktonic mixing and diversity at any depth. Present-day studies on the silica cycle (e.g., Tréguer and De La Rocha, 2013) show that biosiliceous deposits are affected by post-depositional dissolution at the water-sediment interface and during diagenesis. Last but not least, evidences supporting a rise of the OMZ in Dongpan are lacking.

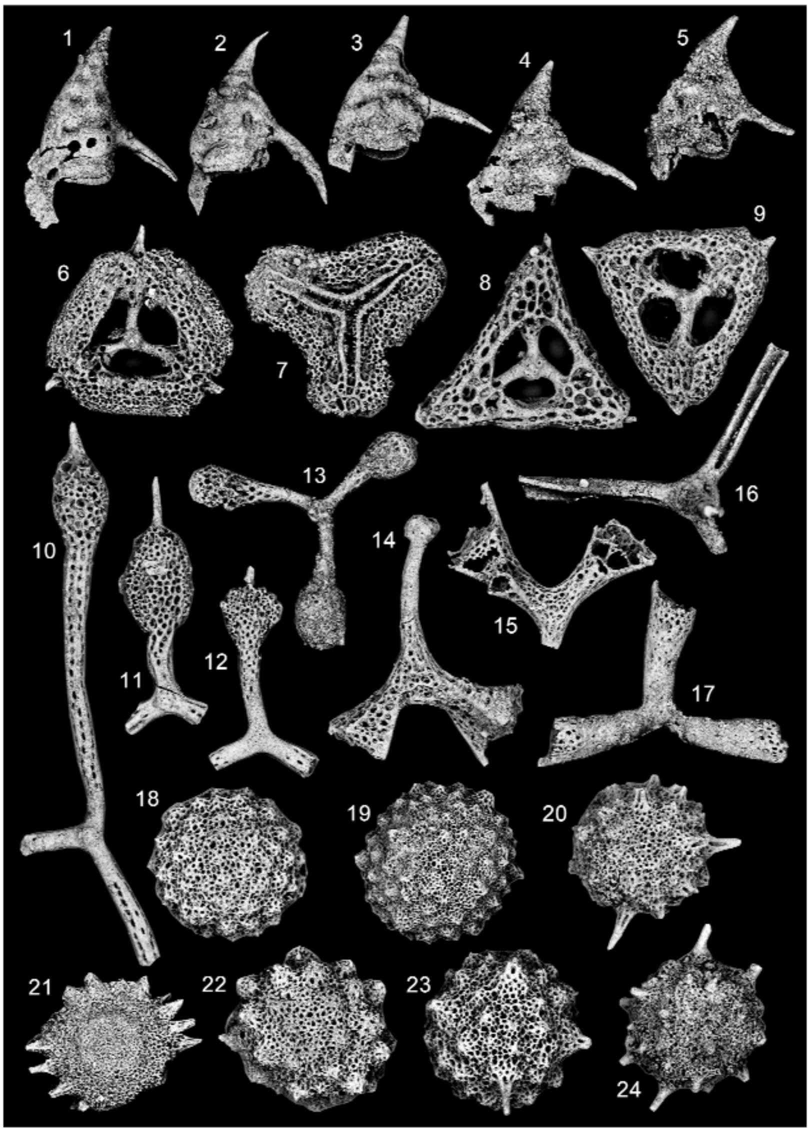

Figure S5. Plate of Dongpan radiolarians ordered by taxon, sample, database number, and maximum dimension. 1) Albaillella yaoi Kuwahara, DGP-2, n°20, 200 µm. 2) Albaillella triangularis Ishiga, Kito & Imoto, DGP-2, n° 21, 210 µm. 3) Albaillella triangularis Ishiga, Kito & Imoto, DGP-1, n°06, 170 µm. 4) Albaillella triangularis Ishiga, Kito & Imoto, DGP-1, n° 11, 190 µm. 5) Albaillella levis

Ishiga, Kito & Imoto, DGP-1, n°07, 190 µm. 6) Foremanhelena circula Shang, Caridroit & Wang, DGP-2, n°02, 260 µm. 7) Triplanospongos musashiensis Sashida & Tonishi, DGP-2, n°03, 260 µm. 8) Foremanhelena robusta Feng, DGP-2, n°05, 220 µm. 9) Foremanhelena robusta Feng, DGP-2, n°12, 230 µm. 10) Ishigaum tristylum Feng, DGP-2, n°11, 700 µm. 11) Ishigaum fusinum Feng, DGP-2, n°10, 400 µm. 12) Ishigaum sp., DGP-2, n°13, 270 µm. 13) Cauletella delicata Caridroit & Shang, DGP-5, n°03, 260 µm. 14) Cauletella paradoxa Shang, Caridroit & Wang, DGP-2, n°07, 400 µm. 15) Cauletella paradoxa Shang, Caridroit & Wang, DGP-2, n°09, 300 µm. 16) Nazarovella gracilis De Wever & Caridroit, DGP-5, n°04, 350 µm. 17) Cauletella manica De Wever & Caridroit, DGP-2, n°14, 210 µm. 18) Hegleria mammilla Sheng & Wang, DGP-2, n°30, 290 µm. 19) Hegleria sp. aff. mammilla Sheng & Wang, DGP-5, n°15, 300 µm. 20) Paracopycintra ziyunensis Feng & Gu, DGP-5, n°18, 270 µm. 21) Copicyntroides sp., DGP-5, n°01, 310 µm. 22) Paracopycintra sp., DGP-5, n°12, 300 µm. 23) Paracopycintra akikawaensis Sashida & Tonishi, DGP-2, n°36, 280 µm. 24) Paracopycintra akikawaensis Sashida & Tonishi, DGP-2, n°33, 300 µm.

Feng, Q.L., and Algeo, T.J.: Evolution of oceanic redox conditions during the Permo-Triassic transition: Evidence from deepwater radiolarian facies. Earth-Sci. Rev., 137, 34–51, doi:10.1016/j.earscirev.2013.12.003, 2014.

Feng, Q.L., He, W.H., Gu, S.Z., Meng, Y.Y., Jin, Y.X., and Zhang, F.: Radiolarian evolution during the latest Permian in South China. Global Planet. Change, 55, 177–192, doi:10.1016/j.gloplacha.2006.06.012, 2007.

He, W.H., Shi, G.R., Feng, Q.L., Campi, M.J., Gu, S.Z., Bu, J.J., Peng, Y.Q., and Meng, Y.Y.: Brachiopod miniaturization and its possible causes during the Permian-Triassic crisis in deep water environments, South China. Palaeogeogr. Palaeocl., 252, 145–163, doi:10.1016/j.palaeo.2006.11.040, 2007.

Shen, J., Algeo, T.J., Zhou, L., Feng, Q., Yu, J., and Ellwood, B.: Volcanic perturbations of the marine environment in South China preceding the latest Permian mass extinction and their biotic effects. Geobiology, 10, 82–103, 2012.

Tréguer, P.J., and De La Rocha, C.L.: The world ocean silica cycle. Annu. Rev. Mar. Sci., 5, 477–501, doi:10.1146/annurev-marine-121211-172346, 2013.

Yin, H.F., Feng, Q.L., Lai, X.L., Baud, A., and Tong, J.N.: The protracted Permo-Triassic crisis and multi-episode extinction around the Permian-Triassic boundary. Global Planet. Change, 55, 1–20, doi:10.1016/j.gloplacha.2006.06.005, 2007.

Zhang, F., Feng, Q.I., Meng, Y.Y., He, W.H., and Gu, S.Z.: Stratigraphy of organic carbon isotope and associated events across the Permian and Triassic boundary in the Dongpan deepwater section in Liuqiao area, Guangxi, South China. Geoscience, 20, 1, 42–48, 2006.

Supplement S5: Penglaitan conodonts